On the performance of Shewhart-type synthetic and runs-rules charts combined with an $\bar{X}$ chart

Sandile Charles Shongwe* **and Marien Alet Graham**
Department of Statistics
University of Pretoria
South Africa

Abstract

A synthetic $\bar{X}$ chart is a combination of a conforming run-length chart and an $\bar{X}$ chart, or equivalently, a *2-of-*(*H+1*) runs-rules (RR) chart with a head-start feature. However, a synthetic $\bar{X}$ chart combined with an $\bar{X}$ chart is called a Synthetic-$\bar{X}$ chart. In this article, we build a framework for Shewhart Synthetic-$\bar{X}$ and improved RR (i.e. *1-of-1* or *2-of-*(*H+1*) without head-start) charts by conducting an in-depth zero-state and steady-state study to gain insight into the design of different classes of these schemes and their performance using the Markov chain imbedding technique. More importantly, we propose a modified side-sensitive Synthetic-$\bar{X}$ chart, and then using overall performance measures we show that this new chart has a uniformly better performance than its Shewhart competitors. We also provide easy to use tables for each of the chart's design parameters to aid practical implementation. Moreover, a performance comparison with their corresponding counterparts (i.e. synthetic $\bar{X}$ and RR charts) is conducted.

Keywords: Extra quadratic loss, Runs-rules, Steady-state, Synthetic chart, Zero-state

1. Introduction

In statistical process control and monitoring (SPCM) field, control charts are usually used to distinguish between the chance and the assignable causes of variation. When a process has only chance causes of variation present, it is said to be statistically in-control (IC), otherwise, the process is said to be out-of-control (OOC). Assume that $\{X_{ij}: i \geq 1; j = 1, 2,\ldots, n\}$ is a sequence of samples from iid $N(\mu_0, \sigma_0^2)$ distribution where μ_0 and σ_0^2 are the specified IC mean and variance, respectively. Let $\bar{X}_i$ denote the plotting statistic calculated from $\{X_{ij}\}$ at sampling point i. A Shewhart control chart that is usually used to monitor $\bar{X}_i$ is called the $\bar{X}$ chart and it signals when a single plotting statistic falls above the upper control limit (*UCL*) or below the lower control limit (*LCL*) which are given by

$$UCL = \mu_0 + k\sigma_0, CL = \mu_0, LCL = \mu_0 - k\sigma_0, \quad (1)$$

where k is the distance of the control limits from the center line (*CL*).

A Shewhart $\bar{X}$ chart is known to be more effective in detecting (sudden) large process shifts in the process mean, however, it is poor in detecting small and moderate mean shifts. Hence, there has been a variety of alternative control charts proposed in the literature to efficiently monitor the process mean. Amongst the most popular control charts, we point out a few; these are cumulative sum (CUSUM), exponentially weighted moving average (EWMA) and control charts based on the change point model. In order to further increase the sensitivity of Shewhart, CUSUM and EWMA $\bar{X}$

* Corresponding author: SC Shongwe (sandile.shongwe@up.ac.za)

charts, various adaptations and generalizations of these basic charts have been considered, for example, the variable sampling interval, variable sample size, variable sample size and interval, variable parameter, double sampling, supplementing runs-rules (RR) and integrating these schemes with other monitoring schemes; see for instance Celano et al.[1], Reynolds and Arnold[2], Daudin[3], Koutras et al.[4], Scariano and Calzada[5], Costa[6], Wu and Spedding[7], Khoo et al.[8], Abbas et al.[9,10], Haq et al.[11], etc. In this paper, we concentrate on the two latter adaptations i.e. the supplementary RR schemes and integrating the Shewhart $\bar{X}$ scheme with the conforming run-length (CRL) scheme – called a synthetic chart; we discuss these two next.

Firstly, a "run" is defined as an uninterrupted sequence of the same elements bordered at each end by other types of elements, see Balakrishnan and Koutras[12]. Koutras et al.[4] gave a literature review on Shewhart-type charts with supplementary RR to improve an $\bar{X}$ chart in detecting small shifts. Most notable of these, is the paper by Klein[13], where the author proposed two powerful rules that improved the ability of the $\bar{X}$ chart to detect small shifts, by means of a Markov chain approach, whereby the control limits in Equation (1) can be adjusted to give the desired ARL_0. The two rules suggested by Klein[13] are the *2-of-2* and *2-of-3*. Later, Acosta-Mejia[14] studied the general form of these rules i.e. *w-of-*(*w*+*v*) where $w \geq 2$ and $v \geq 0$ are specified positive integers. Note that both Klein[13] and Acosta-Mejia[14] showed that these rules require at least *w* plotting statistics before an OOC event can be observed, hence, the $\bar{X}$ chart is more effective than these rules in detecting large shifts as it requires 1 plotting statistic to issue a signal. Thus, to increase the performance of the rules in Klein[13], Khoo and Ariffin[15] proposed two improved runs-rules (IRR) $\bar{X}$ schemes which are a combination of the basic $\bar{X}$ chart and the two rules of Klein[13] i.e. *1-of-1* or *2-of-2* and *1-of-1* or *2-of-3*. Then, Acosta-Mejia[14] studied the general form of the Khoo and Ariffin[15] rules i.e. *1-of-1* or *w-of-*(*w*+*v*), which signal an OOC event when one plotting statistic falls beyond either the *LCL* or *UCL*; or when *w* out of *w*+*v* plotting statistics fall in between the *UCL* (*LCL*) and upper (lower) warning limits (i.e. *UWL* (*LWL*)), respectively. That is, the limits of the IRR $\bar{X}$ scheme are given by

$$UCL = \mu_0 + k_1\sigma_0,\ UWL = \mu_0 + k_2\sigma_0,\ CL = \mu_0,\ LWL = \mu_0 - k_2\sigma_0,\ LCL = \mu_0 - k_1\sigma_0 \qquad (2)$$

where k_1 and k_2 are the distances of the control and warning limits from the *CL*, respectively, with $k_1 > k_2$. Khoo and Ariffin[15] showed that the IRR retains the small shift sensitivity of the rules in Klein[13] and has a better performance for large shifts compared to the Klein[13] rules.

Secondly, a synthetic $\bar{X}$ chart to monitor the process mean consists of two sub-charts, one, a basic $\bar{X}$ chart and a second, a *CRL* chart. For a synthetic chart, an OOC signal is not based on a single plotting statistic falling beyond the control limits in Equation (1), instead, when a sample produces a value beyond the control limits in Equation (1), that sample is marked as nonconforming and the control procedure moves to the second sub-chart and a signal is obtained depending on the

outcome of the *CRL* sub-chart. Note that when a sample produces a value falling between *LCL* and *UCL*, then that sample is marked as conforming. Bourke[16] defined a *CRL* as the number of conforming samples between two consecutive nonconforming samples, inclusive of the nonconforming sample at the end. The *CRL* chart signals when an observed *CRL* value is less than or equal to some threshold, say *H* (an integer, greater or equal to 1), which is defined to be the threshold / control limit of the *CRL* chart. To make the run-length analysis of the synthetic chart easier, Davis and Woodall[17] showed that a synthetic chart is a special case of a RR chart i.e. a *2-of-*(*H*+1) with a head-start (HS) feature. The HS feature implies that we assume that (at time 0) the first observation is nonconforming, consequently, we need at least one other nonconforming sample within the next *H* sampling points, for a *2-of-*(*H*+1) runs-type chart to issue a signal. Similar to Khoo and Ariffin[15], Wu et al.[18] improved the sensitivity of the synthetic $\bar{X}$ chart of Wu and Spedding[7] to efficiently monitor both small and large shifts called a Synthetic-$\bar{X}$ chart. A Synthetic-$\bar{X}$ chart consists of two sub-charts, one, a synthetic $\bar{X}$ chart and second, a basic $\bar{X}$ chart. An OOC signal is observed when one plotting statistic falls beyond either the *LCL* or *UCL* in Equation (2); or when $CRL \leq H$.

The performance of the RR and synthetic $\bar{X}$ charts based on Equation (1) have been investigated and reported in Shongwe and Graham[19]. The focus of this paper is on the performance of the IRR and Synthetic-$\bar{X}$ charts with the limits in Equation (2) – these are summarized in Table I. For these charts, when a sample produces a value between the *UCL* (*LCL*) and *UWL* (*LWL*), that sample is marked as nonconforming, whereas, a value between the *UWL* and *LWL* is marked as conforming.

Table I: Types of IRR and Synthetic-$\bar{X}$ charts

IRR $\bar{X}$ charts	Synthetic-$\bar{X}$ charts
(i) Non-side-sensitive (NSS) *1-of-1* or *w-of-*(*w*+*v*): • Discussed here – (IRR1)	(i) NSS *1-of-1* or *2-of-*(*H*+1): • Wu et al.[18] – (SC1)
(ii) Standard side-sensitive (SSS) *1-of-1* or *w-of-*(*w*+*v*): • Khoo and Ariffin[15] – (IRR2)	(ii) SSS *1-of-1* or *2-of-*(*H*+1): • Discussed here – (SC2)
(iii) Revised side-sensitive (RSS) *1-of-1* or *w-of-*(*w*+*v*): • Discussed here – (IRR3)	(iii) RSS *1-of-1* or *2-of-*(*H*+1): • Machado and Costa[21] – (SC3)
(iv) Modified side-sensitive (MSS) *1-of-1* or *w-of-*(*w*+*v*): • Antzoulakos and Rakitzis[22] – (IRR4)	(iv) MSS *1-of-1* or *2-of-*(*H*+1): • Proposed in this paper – (SC4)

Firstly, there are four types of IRR $\bar{X}$ schemes that are based on the limits in Equation (2) which are as follows:

(i) the NSS *1-of-1* or *w-of-*(*w*+*v*) (adopted from Derman and Ross[20] – denoted by IRR1) with the charting regions shown in Figure 1(a). Hence, IRR1 gives an OOC signal when either one plotting statistic falls on the action region (i.e. region E), or when *w* nonconforming

Table V: The zero-state and steady-state OOC *ARL* values of the *1-of-1* or *2-of-*(H+1) IRR and Synthetic-$\bar{X}$ charts when H = 1, δ_{max} = 5 and ARL_0 = 370.4

		Zero-state				Steady-state	
		IRR1	IRR2, IRR3, IRR4	SC1	SC2, SC3, SC4	IRR1, SC1	IRR2, IRR3, IRR4, SC2, SC3, SC4
	k_1	3.2	3.3	3.4	3.7	3.2	3.3
	k_2	2.0700	1.8756	2.0014	1.8167	2.0705	1.8762
δ	0	370.4	370.4	370.4	370.4	370.4	370.4
	0.1	352.10	343.56	352.32	**341.14**	352.06	**343.53**
	0.2	305.31	280.70	305.65	**274.03**	305.24	**280.64**
	0.3	246.93	212.25	246.66	**203.01**	246.83	**212.16**
	0.4	190.96	155.04	189.46	**145.31**	190.83	**154.93**
	0.5	144.09	112.30	141.32	**103.22**	143.95	**112.18**
	0.6	107.61	81.74	103.91	**73.72**	107.47	**81.62**
	0.7	80.28	60.17	76.10	**53.24**	80.14	**60.05**
	0.8	60.19	44.91	55.88	**38.99**	60.05	**44.80**
	0.9	45.50	34.04	41.33	**28.97**	45.38	**33.93**
	1	34.78	26.20	30.88	**21.85**	34.66	**26.10**
	1.1	26.90	20.49	23.34	**16.73**	26.80	**20.40**
	1.2	21.08	16.26	17.87	**13.01**	20.99	**16.18**
	1.3	16.74	13.11	13.87	**10.26**	16.66	**13.03**
	1.4	13.47	10.72	10.91	**8.21**	13.40	**10.65**
	1.5	10.99	8.89	8.70	**6.67**	10.92	**8.83**
	1.6	9.08	7.47	7.04	**5.49**	9.02	**7.41**
	1.7	7.60	6.36	5.77	**4.58**	7.54	**6.31**
	1.8	6.44	5.48	4.80	**3.88**	6.39	**5.43**
	1.9	5.52	4.77	4.04	**3.32**	5.47	**4.73**
	2	4.78	4.20	3.45	**2.88**	4.74	**4.16**
	2.1	4.19	3.74	2.98	**2.53**	4.15	**3.70**
	2.2	3.71	3.36	2.61	**2.25**	3.67	**3.33**
	2.3	3.31	3.04	2.31	**2.02**	3.28	**3.01**
	2.4	2.99	2.78	2.07	**1.83**	2.96	**2.75**
	2.5	2.71	2.56	1.87	**1.68**	2.69	**2.53**
	2.6	2.49	2.37	1.71	**1.56**	2.46	**2.34**
	2.7	2.29	2.21	1.58	**1.45**	2.27	**2.19**
	2.8	2.13	2.07	1.47	**1.37**	2.10	**2.05**
	2.9	1.99	1.95	1.38	**1.30**	1.97	**1.93**
	3	1.86	1.85	1.31	**1.24**	1.84	**1.83**
	3.1	1.76	1.75	1.25	**1.19**	**1.74**	**1.74**
	3.2	1.67	1.67	1.20	**1.15**	**1.65**	1.66
	3.3	1.58	1.60	1.16	**1.12**	**1.57**	1.58
	3.4	1.51	1.53	1.13	**1.10**	**1.50**	1.52
	3.5	1.45	1.47	1.10	**1.08**	**1.44**	1.46
	3.6	1.39	1.42	1.08	**1.06**	**1.38**	1.41
	3.7	1.34	1.37	1.06	**1.05**	**1.33**	1.36
	3.8	1.30	1.33	1.05	**1.04**	**1.29**	1.32
	3.9	1.26	1.29	1.04	**1.03**	**1.25**	1.28
	4	1.22	1.25	1.03	**1.02**	**1.22**	1.24
	4.1	1.19	1.22	**1.02**	**1.02**	**1.19**	1.21
	4.2	1.16	1.19	1.02	**1.01**	**1.16**	1.18
	4.3	1.14	1.16	**1.01**	**1.01**	**1.13**	1.16
	4.4	1.12	1.14	**1.01**	**1.01**	**1.11**	1.13
	4.5	1.10	1.12	1.01	**1.00**	**1.10**	1.11
	4.6	1.08	1.10	1.01	**1.00**	**1.08**	1.09
	4.7	1.07	1.08	**1.00**	**1.00**	**1.07**	1.08
	4.8	1.06	1.07	**1.00**	**1.00**	**1.05**	1.07
	4.9	1.04	1.05	**1.00**	**1.00**	**1.04**	1.05
	5	1.04	1.04	**1.00**	**1.00**	**1.03**	1.04
EQL		223.95	200.94	188.83	**161.65**	222.79	**199.82**
ARARL		1.4084	1.2827	1.1499	**1.0000**	1.1004	**1.0000**
PCI		1.3854	1.2430	1.1681	**1.0000**	1.1149	**1.0000**

Table VI: The zero-state and steady-state OOC *ARL* values of the *1-of-1* or *2-of-*(*H*+1) IRR and Synthetic-$\bar{X}$ charts when $H = 5$, $\delta_{max} = 5$ and $ARL_0 = 370.4$

		Zero-state								Steady-state			
		IRR1	IRR2	IRR3	IRR4	SC1	SC2	SC3	SC4	IRR1,SC1	IRR2,SC2	IRR3,SC3	IRR4,SC4
	k_1	3.3	3.3	3.3	3.3	4.0	4.5	4.6	4.6	3.3	3.3	3.4	3.4
	k_2	2.3105	2.1891	2.1842	2.0053	2.2645	2.1426	2.1369	1.9383	2.3119	2.1907	2.1577	1.9752
δ	0	370.4	370.3	370.4	370.4	370.3	370.3	370.3	**370.3**	370.5	370.4	370.4	**370.3**
	0.1	350.52	340.37	340.05	336.56	349.68	334.93	334.28	**330.02**	350.47	340.42	338.59	**334.69**
	0.2	300.04	272.16	271.21	261.74	296.98	257.71	256.12	**245.45**	299.85	272.10	267.50	**257.28**
	0.3	238.21	200.92	199.70	186.97	231.95	181.82	179.96	**166.77**	237.88	200.76	195.06	**181.66**
	0.4	180.36	143.78	142.61	129.59	171.15	124.39	122.75	**110.21**	179.93	143.55	138.23	**124.81**
	0.5	133.26	102.53	101.57	89.80	122.24	84.94	83.67	**73.02**	132.79	102.27	97.91	**85.98**
	0.6	97.68	73.84	73.09	63.09	86.10	58.64	57.71	**49.13**	97.20	73.57	70.21	**60.19**
	0.7	71.80	54.02	53.46	45.23	60.59	41.15	40.48	**33.75**	71.34	53.76	51.24	**43.08**
	0.8	53.26	40.25	39.83	33.18	42.96	29.42	28.95	**23.72**	52.84	40.00	38.14	**31.58**
	0.9	40.04	30.56	30.25	24.91	30.85	21.46	21.12	**17.08**	39.65	30.32	28.96	**23.72**
	1	30.57	23.64	23.41	19.15	22.52	15.97	15.73	**12.61**	30.22	23.43	22.42	**18.25**
	1.1	23.72	18.63	18.46	15.05	16.74	12.13	11.96	**9.54**	23.41	18.43	17.69	**14.37**
	1.2	18.72	14.94	14.81	12.08	12.69	9.40	9.28	**7.39**	18.44	14.76	14.21	**11.56**
	1.3	15.01	12.18	12.08	9.89	9.81	7.43	7.34	**5.86**	14.76	12.02	11.61	**9.48**
	1.4	12.23	10.08	10.01	8.25	7.73	5.99	5.93	**4.76**	12.01	9.94	9.63	**7.93**
	1.5	10.12	8.47	8.41	6.99	6.22	4.93	4.88	**3.94**	9.92	8.34	8.11	**6.74**
	1.6	8.49	7.22	7.17	6.01	5.09	4.12	4.09	**3.34**	8.31	7.10	6.93	**5.81**
	1.7	7.22	6.22	6.19	5.24	4.25	3.51	3.48	**2.88**	7.05	6.11	5.99	**5.08**
	1.8	6.21	5.43	5.40	4.63	3.61	3.04	3.02	**2.52**	6.06	5.33	5.24	**4.50**
	1.9	5.41	4.79	4.77	4.13	3.12	2.67	2.65	**2.24**	5.27	4.70	4.64	**4.03**
	2	4.76	4.26	4.24	3.72	2.73	2.38	2.37	**2.03**	4.64	4.18	4.14	**3.64**
	2.1	4.23	3.83	3.81	3.38	2.43	2.15	2.14	**1.85**	4.11	3.75	3.73	**3.31**
	2.2	3.79	3.46	3.45	3.09	2.19	1.96	1.95	**1.71**	3.68	3.39	3.38	**3.04**
	2.3	3.42	3.16	3.15	2.85	1.99	1.81	1.80	**1.59**	3.32	3.09	3.09	**2.81**
	2.4	3.11	2.90	2.89	2.64	1.83	1.68	1.67	**1.50**	3.02	2.83	2.85	**2.62**
	2.5	2.85	2.67	2.67	2.46	1.70	1.57	1.57	**1.42**	2.77	2.61	2.63	**2.44**
	2.6	2.62	2.48	2.47	2.31	1.59	1.48	1.48	**1.35**	2.55	2.43	2.45	**2.29**
	2.7	2.43	2.31	2.31	2.17	1.50	1.41	1.40	**1.29**	2.36	2.26	2.29	**2.16**
	2.8	2.26	2.16	2.16	2.05	1.42	1.34	1.34	**1.25**	2.19	2.12	2.15	**2.05**
	2.9	2.11	2.03	2.03	1.94	1.36	1.29	1.29	**1.20**	2.05	1.99	2.02	**1.94**
	3	1.98	1.92	1.92	1.84	1.30	1.24	1.24	**1.17**	1.93	1.88	1.91	**1.85**
	3.1	1.87	1.82	1.81	1.75	1.25	1.20	1.20	**1.14**	1.82	1.78	1.82	**1.77**
	3.2	1.76	1.72	1.72	1.67	1.21	1.17	1.17	**1.12**	1.72	**1.69**	1.73	**1.69**
	3.3	1.67	1.64	1.64	1.60	1.18	1.14	1.14	**1.10**	1.63	**1.61**	1.65	1.62
	3.4	1.59	1.57	1.57	1.54	1.15	1.12	1.12	**1.08**	1.56	**1.54**	1.58	1.56
	3.5	1.52	1.50	1.50	1.48	1.12	1.10	1.09	**1.06**	1.49	**1.48**	1.52	1.50
	3.6	1.46	1.44	1.44	1.42	1.10	1.08	1.08	**1.05**	1.43	**1.42**	1.46	1.45
	3.7	1.40	1.39	1.39	1.38	1.08	1.06	1.06	**1.04**	**1.37**	**1.37**	1.40	1.40
	3.8	1.35	1.34	1.34	1.33	1.07	1.05	1.05	**1.03**	1.33	**1.32**	1.36	1.35
	3.9	1.30	1.30	1.30	1.29	1.05	1.04	1.04	**1.03**	**1.28**	**1.28**	1.31	1.31
	4	1.26	1.26	1.26	1.25	1.04	1.03	1.03	**1.02**	**1.24**	**1.24**	1.27	1.27
	4.1	1.23	1.22	1.22	1.22	1.03	1.03	1.03	**1.02**	**1.21**	**1.21**	1.24	1.24
	4.2	1.19	1.19	1.19	1.19	1.03	1.02	1.02	**1.01**	**1.18**	**1.18**	1.21	1.21
	4.3	1.17	1.16	1.16	1.16	1.02	1.02	1.02	**1.01**	**1.15**	**1.15**	1.18	1.18
	4.4	1.14	1.14	1.14	1.14	1.02	**1.01**	**1.01**	**1.01**	**1.13**	**1.13**	1.15	1.15
	4.5	1.12	1.12	1.12	1.12	**1.01**	**1.01**	**1.01**	**1.01**	**1.11**	**1.11**	1.13	1.13
	4.6	1.10	1.10	1.10	1.10	1.01	1.01	1.01	**1.00**	**1.09**	**1.09**	1.11	1.11
	4.7	1.08	1.08	1.08	1.08	1.01	1.01	1.01	**1.00**	**1.08**	**1.08**	1.09	1.09
	4.8	1.07	1.07	1.07	1.07	1.01	**1.00**	**1.00**	**1.00**	**1.06**	**1.06**	1.08	1.08
	4.9	1.06	1.06	1.06	1.06	**1.00**	**1.00**	**1.00**	**1.00**	**1.05**	**1.05**	1.06	1.06
	5	1.04	1.04	1.04	1.04	**1.00**	**1.00**	**1.00**	**1.00**	**1.04**	**1.04**	1.05	1.05
EQL		219.02	197.24	196.50	181.79	166.89	145.41	144.62	**133.24**	215.70	194.88	194.11	**180.08**
ARARL		1.7686	1.5852	1.5789	1.4432	1.2797	1.1078	1.1014	**1.0000**	1.2072	1.0886	1.0834	**1.0000**
PCI		1.6438	1.4803	1.4748	1.3643	1.2525	1.0913	1.0854	**1.0000**	1.1978	1.0822	1.0779	**1.0000**

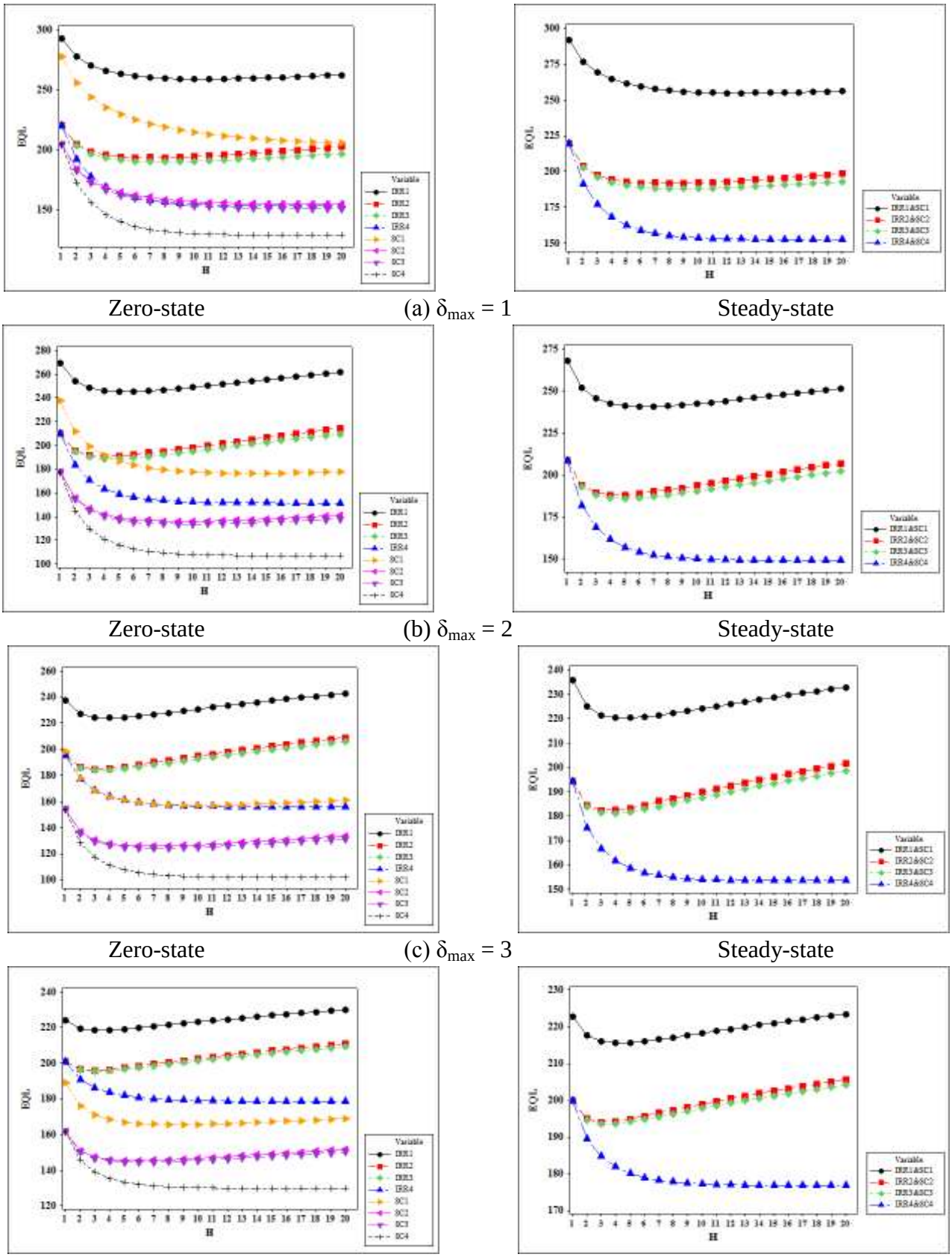

Zero-state (a) $\delta_{max} = 1$ Steady-state

Zero-state (b) $\delta_{max} = 2$ Steady-state

Zero-state (c) $\delta_{max} = 3$ Steady-state

Zero-state (d) $\delta_{max} = 5$ Steady-state

Figure 2: The zero-state and steady-state *EQL* values of the *1-of-1* or *2-of-*(*H*+1) IRR and Synthetic-$\bar{X}$ charts when $H = 1, 2, \ldots, 20$ for an $ARL_0 = 370.4$

Next, we investigate whether the SC4 scheme has a uniformly better overall OOC performance as *H* varies from 1 to 20 by plotting the values of the minimum ZS and SS *EQL* for

each scheme listed in Table I (similar to those in Tables V and VI). It is clear from Figure 2 that the SC4 scheme outperform all the other schemes once $H > 1$, both in ZS and SS modes for a variety of δ_{max} values. Moreover, the convergence of k_2 values as H increases for the SC4 and IRR4 schemes result in the convergence of their *EQL* values. The *EQL* values of the IRR2 and IRR3 as well as SC2 and SC3 schemes are almost equal, however, with those of the IRR3 and SC3 just slightly better. The IRR1 scheme is the worst performing scheme and the SC1 scheme become less effective as δ_{max} decrease. For each of the schemes, we recommend a value of H that corresponds to the minimum of the *EQL* curve depending on the desired δ_{max}. The results in Figure 2 are further illustrated by the results in Tables VII and VIII when $\delta_{max} = 5$. That is, we see that the *PCI*s and *ARARL*s of the IRR2 and IRR3 as well as SC2 and SC3 schemes are relatively close to each other. Also, IRR1 has the worst performance, for instance, when $H = 5$, it is 64.38% and 76.86% worse than the SC4 scheme in ZS with respect to the *PCI* and *ARARL*, respectively. The *PCI*s and *ARARL*s of the SC4 scheme have a uniformly better performance with equality in performance occurring only when $H = 1$ and with the IRR4 in SS.

Table VII: The zero-state and steady-state *PCI* values of the *1-of-1* or *2-of-*(H+1) IRR and Synthetic-$\bar{X}$ charts for $\delta_{max} = 5$ when $H = 1, 2, \ldots, 20$ and $ARL_0 = 370.4$

	Zero-state								Steady-state			
H	IRR1	IRR2	IRR3	IRR4	SC1	SC2	SC3	SC4	IRR1&SC1	IRR2&SC2	IRR3&SC3	IRR4&SC4
1	1.3854	1.2430	1.2430	1.2430	1.1681	1.0000	1.0000	1.0000	1.1149	1.0000	1.0000	1.0000
2	1.5057	1.3485	1.3463	1.3107	1.2088	1.0358	1.0332	1.0000	1.1485	1.0283	1.0267	1.0000
3	1.5719	1.4099	1.4063	1.3405	1.2300	1.0606	1.0565	1.0000	1.1694	1.0507	1.0481	1.0000
4	1.6144	1.4510	1.4463	1.3559	1.2435	1.0783	1.0732	1.0000	1.1853	1.0683	1.0648	1.0000
5	1.6438	1.4803	1.4748	1.3643	1.2525	1.0913	1.0854	1.0000	1.1978	1.0822	1.0779	1.0000
6	1.6653	1.5023	1.4959	1.3692	1.2589	1.1012	1.0946	1.0000	1.2072	1.0931	1.0883	1.0000
7	1.6817	1.5215	1.5123	1.3721	1.2636	1.1112	1.1020	1.0000	1.2149	1.1034	1.0969	1.0000
8	1.6944	1.5334	1.5256	1.3737	1.2673	1.1157	1.1081	1.0000	1.2213	1.1097	1.1041	1.0000
9	1.7050	1.5451	1.5369	1.3748	1.2705	1.1214	1.1133	1.0000	1.2267	1.1164	1.1104	1.0000
10	1.7138	1.5554	1.5464	1.3753	1.2734	1.1266	1.1181	1.0000	1.2314	1.1223	1.1159	1.0000
11	1.7215	1.5645	1.5550	1.3757	1.2762	1.1314	1.1226	1.0000	1.2356	1.1275	1.1209	1.0000
12	1.7286	1.5726	1.5627	1.3758	1.2789	1.1360	1.1268	1.0000	1.2395	1.1324	1.1256	1.0000
13	1.7350	1.5804	1.5700	1.3760	1.2817	1.1404	1.1309	1.0000	1.2430	1.1369	1.1299	1.0000
14	1.7409	1.5874	1.5767	1.3760	1.2844	1.1446	1.1348	1.0000	1.2464	1.1412	1.1339	1.0000
15	1.7468	1.5943	1.5832	1.3761	1.2873	1.1490	1.1388	1.0000	1.2496	1.1453	1.1377	1.0000
16	1.7521	1.6009	1.5893	1.3761	1.2902	1.1531	1.1427	1.0000	1.2527	1.1491	1.1413	1.0000
17	1.7573	1.6071	1.5951	1.3761	1.2931	1.1572	1.1465	1.0000	1.2557	1.1528	1.1448	1.0000
18	1.7622	1.6130	1.6007	1.3761	1.2961	1.1613	1.1503	1.0000	1.2585	1.1564	1.1481	1.0000
19	1.7670	1.6189	1.6061	1.3761	1.2991	1.1652	1.1540	1.0000	1.2612	1.1600	1.1513	1.0000
20	1.7716	1.6244	1.6113	1.3761	1.3021	1.1692	1.1578	1.0000	1.2638	1.1631	1.1544	1.0000

Table VIII: The zero-state and steady-state *ARARL* values of the *1-of-1* or *2-of-*(*H*+1) IRR and Synthetic-$\bar{X}$ charts for $\delta_{max} = 5$ when $H = 1, 2, \ldots, 20$ and $ARL_0 = 370.4$

	Zero-state								Steady-state			
H	IRR1	IRR2	IRR3	IRR4	SC1	SC2	SC3	SC4	IRR1&SC1	IRR2&SC2	IRR3&SC3	IRR4&SC4
1	1.4084	1.2827	1.2827	1.2827	1.1499	1.0000	1.0000	1.0000	1.1004	1.0000	1.0000	1.0000
2	1.5651	1.4095	1.4073	1.3686	1.2040	1.0377	1.0352	1.0000	1.1393	1.0277	1.0262	1.0000
3	1.6603	1.4887	1.4849	1.4090	1.2381	1.0674	1.0632	1.0000	1.1694	1.0523	1.0497	1.0000
4	1.7230	1.5443	1.5391	1.4308	1.2624	1.0902	1.0848	1.0000	1.1906	1.0724	1.0683	1.0000
5	1.7686	1.5852	1.5789	1.4432	1.2797	1.1078	1.1014	1.0000	1.2072	1.0886	1.0834	1.0000
6	1.8024	1.6166	1.6091	1.4505	1.2924	1.1218	1.1146	1.0000	1.2199	1.1015	1.0955	1.0000
7	1.8315	1.6436	1.6328	1.4549	1.3021	1.1355	1.1253	1.0000	1.2301	1.1136	1.1055	1.0000
8	1.8517	1.6613	1.6520	1.4575	1.3096	1.1428	1.1343	1.0000	1.2312	1.1173	1.1109	1.0000
9	1.8682	1.6780	1.6682	1.4591	1.3159	1.1512	1.1421	1.0000	1.2380	1.1249	1.1181	1.0000
10	1.8819	1.6927	1.6821	1.4600	1.3216	1.1588	1.1493	1.0000	1.2437	1.1317	1.1244	1.0000
11	1.8936	1.7057	1.6943	1.4607	1.3267	1.1659	1.1559	1.0000	1.2488	1.1376	1.1301	1.0000
12	1.9041	1.7172	1.7054	1.4609	1.3316	1.1726	1.1621	1.0000	1.2536	1.1433	1.1362	1.0000
13	1.9137	1.7281	1.7157	1.4611	1.3364	1.1790	1.1682	1.0000	1.2578	1.1484	1.1411	1.0000
14	1.9223	1.7380	1.7252	1.4612	1.3411	1.1852	1.1740	1.0000	1.2618	1.1532	1.1456	1.0000
15	1.9308	1.7476	1.7343	1.4614	1.3458	1.1913	1.1798	1.0000	1.2655	1.1578	1.1499	1.0000
16	1.9385	1.7567	1.7428	1.4614	1.3505	1.1973	1.1854	1.0000	1.2691	1.1621	1.1540	1.0000
17	1.9459	1.7654	1.7509	1.4614	1.3552	1.2031	1.1910	1.0000	1.2726	1.1663	1.1579	1.0000
18	1.9529	1.7735	1.7587	1.4614	1.3599	1.2089	1.1964	1.0000	1.2757	1.1703	1.1616	1.0000
19	1.9598	1.7816	1.7662	1.4615	1.3645	1.2145	1.2017	1.0000	1.2789	1.1743	1.1652	1.0000
20	1.9662	1.7892	1.7734	1.4615	1.3691	1.2201	1.2070	1.0000	1.2818	1.1778	1.1687	1.0000

4. Comparison with the *2-of-*(*H*+1) runs-rules and synthetic $\bar{X}$ charts

In this section, we compare the overall performance of the schemes in Table I with their corresponding counterparts that are based on Equation (1) which are discussed in Shongwe and Graham[19]. As explained in Figure 1, the synthetic-type and runs-type charts may be classed into four categories i.e. NSS, SSS, RSS and MSS. The NSS, SSS, RSS, MSS synthetic $\bar{X}$ charts were proposed by Wu and Spedding[7], Davis and Woodall[17], Machado and Costa[26], Shongwe and Graham[19] – these are denoted by S1, S2, S3, S4, respectively. The NSS, SSS, RSS, MSS *2-of-*(*H*+1) RR $\bar{X}$ charts were proposed by Derman and Ross[20], Klein[13], adopted from Machado and Costa[26], Antzoulakos and Rakitzis[29] – these are denoted by RR1, RR2, RR3, RR4, respectively.

In Figure 3, the ZS and SS *EQL*s of these schemes are compared with those listed in Table I when $\delta_{max} = 5$ and we overlaid the *EQL* value of 253.99 of the $\bar{X}$ chart to measure its performance against these schemes. We see that in ZS, the Synthetic-$\bar{X}$ and synthetic $\bar{X}$ charts have an almost equal *EQL* values, with the Synthetic-$\bar{X}$ having just slightly lower *EQL*s. Hence, in ZS it follow that it is better to use the more effective one-sided Synthetic-$\bar{X}$ discussed in Wu et al.[18] rather than the two-sided Synthetic-$\bar{X}$ chart discussed here. However, in SS, there is a significant difference between the Synthetic-$\bar{X}$ and synthetic $\bar{X}$ charts with SC1, SC2, SC3 and SC4 having a better performance than the S1, S2, S3 and S3 schemes, respectively. For RR and IRR schemes, there is a significant performance difference especially when δ_{max} is large, with the IRR1, IRR2, IRR3 and IRR4 better than the RR1, RR2, RR3 and RR4, respectively. Note that as δ_{max} decrease, the *EQL*

values of the IRR and RR schemes become closer to each other, respectively. Finally, the $\bar{X}$ chart outperform some of the RR schemes, however, as δ_{max} decrease, it becomes less effective.

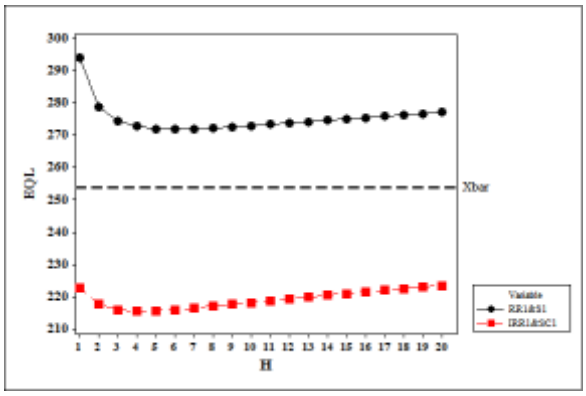

Zero-state (a) NSS Steady-state

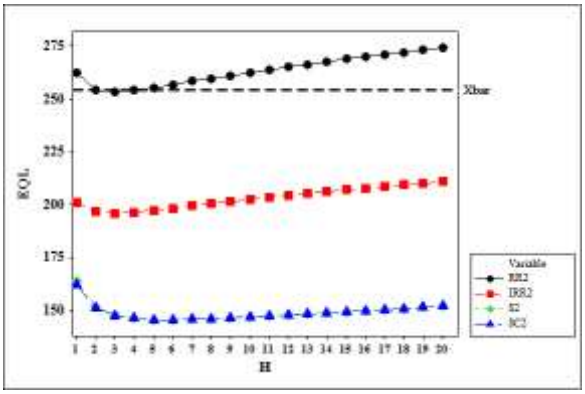

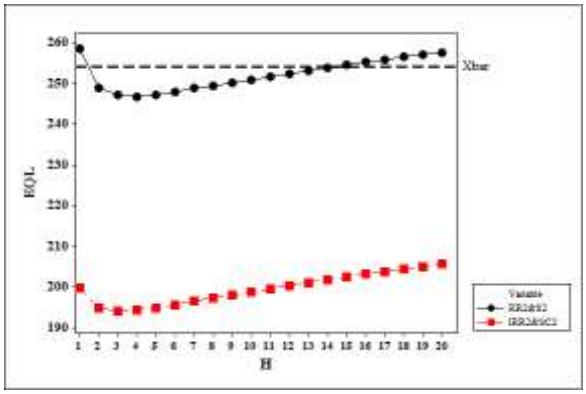

Zero-state (b) SSS Steady-state

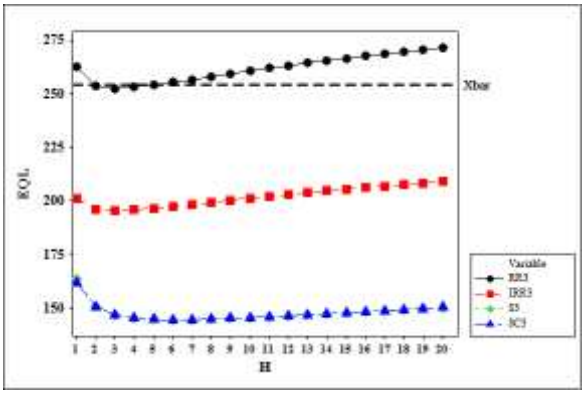

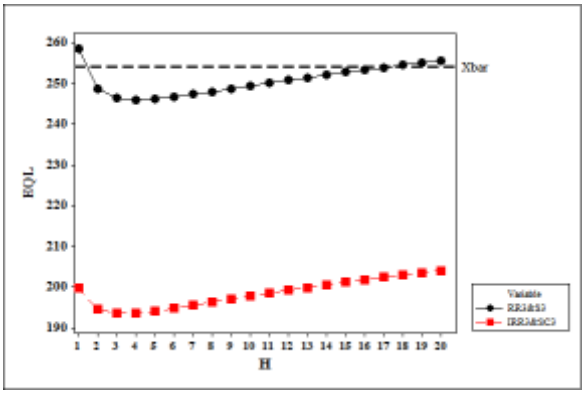

Zero-state (c) RSS Steady-state

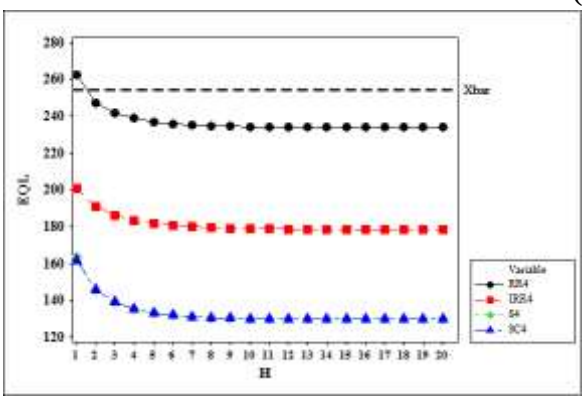

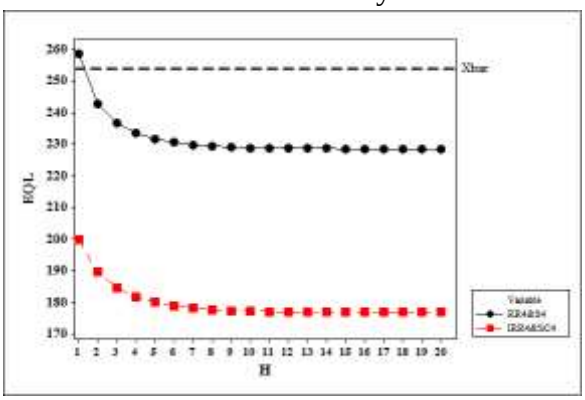

Zero-state (d) MSS Steady-state

Figure 3: Comparison of the *EQL* values of the IRR and Synthetic- $\bar{X}$ charts with the RR and synthetic $\bar{X}$ charts when $H = 1, 2, \ldots, 20$ for $ARL_0 = 370.4$ and $\delta_{max} = 5$

5. Conclusion

In this paper, we proposed a MSS Synthetic-$\bar{X}$ (i.e. SC4) chart using a Markov chain imbedding technique and compared its ZS and SS *ARL*, *EQL*, *PCI* and *ARARL* performance with its seven Shewhart-type competitors. The convergence in the design parameter k_2 as *H* increases for some given k_1 have a direct effect on the specific shift and overall performance of the SC4 chart. Hence, for all values of *H* considered here, the new SC4 scheme yields a uniformly better ZS OOC *ARL*, whereas, in SS, the OOC *ARL* is only better for small and moderate shifts. However, the overall performance measures for the SC4 scheme both in ZS and SS are either the same or better than those of the other schemes discussed here; with equality occurring only when $H = 1$ and with the IRR4 in SS mode. Furthermore, we compared the *EQL* performance of the *1-of-1* or *2-of-*(H+1) IRR and Synthetic-$\bar{X}$ charts with the *2-of-*(H+1) RR and synthetic $\bar{X}$ charts in terms of NSS, SSS, RSS, MSS categories. We observed that there is no significant benefit in adopting the more complicated ZS Synthetic-$\bar{X}$ schemes over ZS synthetic $\bar{X}$ schemes, however, the respective SS Synthetic-$\bar{X}$ schemes have a significant benefit over the SS synthetic $\bar{X}$ schemes.

Note that the results presented here only hold when the observations are from a normal distribution, hence, for other distributions, these will need to be re-evaluated or nonparametric counterparts need to be considered.

Acknowledgements

Part of this work was supported by the SARCHI Chair at the University of Pretoria. Sandile Shongwe's research was supported by National Research Foundation (NRF) Innovation Doctoral Scholarship and Marien Graham's research was supported in part by the National Research Foundation (Thuthuka programme: TTK14061168807, Grant number: 94102).

Appendix

The transition probability matrix (TPM) of the Markov chain for any general (integer) value of $M > 0$ is given by

$$\boldsymbol{P}_{(M+1)\times(M+1)} = \begin{pmatrix} \mathbf{Q}_{(M\times M)} & | & \boldsymbol{r}_{(M\times 1)} \\ - & - & - \\ \mathbf{0}'_{(1\times M)} & | & 1_{(1\times 1)} \end{pmatrix} \tag{8}$$

where $\mathbf{Q}_{(M\times M)}$ is the essential TPM, the vector $\mathbf{r}_{(M\times 1)}$ satisfies $\mathbf{r} = \mathbf{1} - \mathbf{Q1}$ with $\mathbf{1}_{(M\times 1)} = (1\ 1\ \ldots\ 1)^T$ and $\mathbf{0}_{(M\times 1)} = (0\ 0\ \ldots\ 0)^T$. In order to construct the TPM, we follow the Markov chain imbedding technique discussed briefly by Antzoulakos and Rakitzis[22,29], Low et al.[30] and in detail by Fu and Lou[31]. This entails dividing the chart into separate distinct regions (see Figure 1) i.e. let $\{\bar{X}_i; i \geq 1\}$ be a sequence of iid trials taking values in the set ζ_1 = {O, U, E}, ζ_2 = {A, O, D, E} and

ζ_3 = {A, B, C, D, E} for the (IRR1, SC1), (IRR2, SC2, IRR3, SC3) and (IRR4, SC4), respectively. Then, define the probability that a plotting statistic falls in each region:

(i) θ_A denotes the probability that a point falls between the *UWL* and *UCL* i.e. $P(\bar{X}_i \in A)$;

(ii) θ_B denotes the probability that a point falls between the *CL* and *UWL* i.e. $P(\bar{X}_i \in B)$;

(iii) θ_C denotes the probability that a point falls between the *LWL* and *CL* i.e. $P(\bar{X}_i \in C)$;

(iv) θ_D denotes the probability that a point falls between the *LCL* and *LWL* i.e. $P(\bar{X}_i \in D)$;

(v) θ_O=θ_B+θ_C denotes the probability that a point falls between the *LWL* and *UWL* i.e. $P(\bar{X}_i \in O)$;

(vi) θ_U=θ_A+θ_D denotes the probability that a point falls either between the *UWL* and *UCL*, or *LCL* and *LWL* i.e. $P(\bar{X}_i \in U)$;

(vii) θ_E denotes the probability that a point falls either above the *UCL*, or below the *LCL* i.e. $P(\bar{X}_i \in E)$.

For some sample size, *n*, suppose that the values of μ_0 and σ_0^2 are known. Thus the probabilities of a plotting statistic falling in a specific region are given by

$$\begin{aligned}
\theta_A(\delta) &= P(UWL \le \bar{X} < UCL) = \Phi\left(k_1 - \delta\sqrt{n}\right) - \Phi\left(k_2 - \delta\sqrt{n}\right) \\
\theta_B(\delta) &= P(CL \le \bar{X} < UWL) = \Phi\left(k_2 - \delta\sqrt{n}\right) - \Phi\left(-\delta\sqrt{n}\right) \\
\theta_C(\delta) &= P(LWL < \bar{X} \le CL) = \Phi\left(-\delta\sqrt{n}\right) - \Phi\left(-k_2 - \delta\sqrt{n}\right) \\
\theta_D(\delta) &= P(LCL < \bar{X} \le LWL) = \Phi\left(-k_2 - \delta\sqrt{n}\right) - \Phi\left(-k_1 - \delta\sqrt{n}\right) \\
\theta_O(\delta) &= P(LWL < \bar{X} < UWL) = \theta_B(\delta) + \theta_C(\delta) \\
\theta_U(\delta) &= P(UWL \le \bar{X} < UCL) + P(LCL < \bar{X} \le LWL) = \theta_A(\delta) + \theta_D(\delta) \\
\theta_E(\delta) &= P(\bar{X} \ge UCL) + P(\bar{X} \le LCL) = 1 - \Phi\left(k_1 - \delta\sqrt{n}\right) + \Phi\left(-k_1 - \delta\sqrt{n}\right);
\end{aligned} \tag{9}$$

respectively, where $\Phi(\cdot)$ denotes the cumulative distribution function (cdf) of the standard normal distribution and δ is the shift parameter expressed in terms of the standard deviation units and we let *CL* = 0.

Moreover, we need to define the compound patterns that result in an OOC event (which is also known as the waiting time until the first occurrence of an OOC signal). For example, the sequence of plotting statistics 'AA' indicates two consecutive plotting statistics falling in region A, whereas 'ABA' indicates the first plotting statistic falling in region A, the second in region B and the third in region A, etc. The symbol '±' is used to denote the assumption that (at time 0) the first observation falls either on the upper or lower warning region (i.e. HS feature), so that '±A' indicate the first plotting statistic falls either on region A or D and the second on region A. Following Fu and Lou[31], we let the sequences of conforming and nonconforming samples, say $\Lambda_l =$ ABBA, to be the l^{th} simple pattern within a sequence of *n* four-state trials from, say, set ζ_3. Furthermore, let Ψ_r to be r^{th} simple pattern with the sequence of states starting with a HS state, say Ψ_r = {±OOA}. Then, define Λ as a compound pattern if it is the union of ω distinct simple patterns i.e. $\Lambda = \Lambda_1 \cup \Lambda_2 \cup$

$\ldots \cup \Lambda_\omega$. Similarly, define Ψ as a compound pattern if it is the union of υ distinct simple patterns i.e. $\Psi = \Psi_1 \cup \Psi_2 \cup \ldots \cup \Psi_\upsilon$. Let W denote the waiting time for the first occurrence of either Λ or Ψ. Then the run-length distribution of a control chart coincides with the waiting time distribution of W. That is, the run-length distribution of the chart becomes the waiting time until the first occurrence of one of the patterns, $\Lambda_1,\ldots, \Lambda_\omega, \Psi_1,\ldots, \Psi_\upsilon$ and these are the absorbing states of the Markov chain, where $\omega+\upsilon$ denotes the number of patterns (or sequences) of the $\bar{X}_i$ that cause the chart to signal. Then we define the Markov chain with the state space, Ω, operating on $\{\bar{X}_i; i \geq 1\}$ as follows:

- the absorbing state – corresponding to the union of $\Lambda_1,\ldots, \Lambda_\omega, \Psi_1,\ldots, \Psi_\upsilon$; in order to reduce the dimension of the TPM, the $\omega+\upsilon$ absorbing states which signal the entrance of the Markov chain to each of the $\omega+\upsilon$ distinct simple patterns may be substituted by a single absorbing state, denoted by OOC;
- the sub-patterns – corresponding to the distinct first element(s) of the simple pattern $\Lambda_1,\ldots, \Lambda_\omega$ and $\Psi_1,\ldots, \Psi_\upsilon$ without the last element. These sub-patterns are non-absorbing and are denoted by $\eta_1,\ldots, \eta_\tau$ and $\psi_{1,\ldots,}\psi_\kappa$ where $\tau \leq \omega$ and $\kappa < \upsilon$, respectively, with one of these η_i equal to the transient state, denoted by ϕ, corresponding to the IC central region in Figure 1.

For any $H > 0$, the dimension (i.e. M+1) of the TPM in Equation (8) for the schemes listed in Table I are given by

$$\text{IRR1: } (H+1)+1, \quad \text{IRR2: } (H^2+H+1)+1, \quad \text{IRR3: } (2H+1)+1, \quad \text{IRR4: } (2H+1)+1 \tag{10a}$$

and

$$\text{SC1:}(H+1)+1, \text{ SC2:}[(H^2+H+1)+H]+1, \text{ SC3:}[(2H+1)+H]+1, \text{ SC4:}[(2H+1)+(2H-1)]+1, \tag{10b}$$

respectively. That is, M, the dimension of the essential TPM, is given by

$$M = \begin{cases} \tau + \kappa & \text{for SC2, SC3, SC4} \\ \tau & \text{for SC1, IRR1, IRR2, IRR3, IRR4} \end{cases} \tag{11}$$

where

$$\kappa = \begin{cases} H & \text{for SC2, SC3} \\ 2H-1 & \text{for SC4.} \end{cases} \tag{12}$$

Based on this, for any $H > 0$, we define the state spaces as follows

IRR1 & SC1: $\Omega = \{\eta_1 = \phi, \eta_2,\ldots, \eta_\tau; \text{OOC}\}$

IRR2, IRR3, IRR4: $\Omega = \{\eta_1,\ldots, \eta_{\frac{(\tau+1)}{2}-1}, \eta_{\frac{(\tau+1)}{2}} = \phi, \eta_{\frac{(\tau+1)}{2}+1}, \ldots, \eta_\tau; \text{OOC}\}$ (13)

SC2, SC3, SC4: $\Omega = \{\eta_1,\ldots, \eta_{\frac{(\tau+1)}{2}-1}, \eta_{\frac{(\tau+1)}{2}} = \phi, \eta_{\frac{(\tau+1)}{2}+1}, \ldots, \eta_\tau; \psi_1, \ldots, \psi_\kappa; \text{OOC}\}$

In this paper, we considered H = 1, 2,…, 20, hence, in Table IX we show the dimension of the TPMs for each scheme listed in Table I.

Table IX: The dimension (M+1)×(M+1) of the TPM of the embedded Markov chain approach for the *1-of-1* or *2-of-*(H+1) IRR and Synthetic-$\bar{X}$ charts when H = 1,…, 20

H	IRR1	IRR2	IRR3	IRR4	SC1	SC2	SC3	SC4
1	3×3	4×4	4×4	4×4	3×3	5×5	5×5	5×5
2	4×4	8×8	6×6	6×6	4×4	10×10	8×8	9×9
3	5×5	14×14	8×8	8×8	5×5	17×17	11×11	13×13
4	6×6	22×22	10×10	10×10	6×6	26×26	14×14	17×17
5	7×7	32×32	12×12	12×12	7×7	37×37	17×17	21×21
6	8×8	44×44	14×14	14×14	8×8	50×50	20×20	25×25
7	9×9	58×58	16×16	16×16	9×9	65×65	23×23	29×29
8	10×10	74×74	18×18	18×18	10×10	82×82	26×26	33×33
9	11×11	92×92	20×20	20×20	11×11	101×101	29×29	37×37
10	12×12	112×112	22×22	22×22	12×12	122×122	32×32	41×41
11	13×13	134×134	24×24	24×24	13×13	145×145	35×35	45×45
12	14×14	158×158	26×26	26×26	14×14	170×170	38×38	49×49
13	15×15	184×184	28×28	28×28	15×15	197×197	41×41	53×53
14	16×16	212×212	30×30	30×30	16×16	226×226	44×44	57×57
15	17×17	242×242	32×32	32×32	17×17	257×257	47×47	61×61
16	18×18	274×274	34×34	34×34	18×18	290×290	50×50	65×65
17	19×19	308×308	36×36	36×36	19×19	325×325	53×53	69×69
18	20×20	344×344	38×38	38×38	20×20	362×362	56×56	73×73
19	21×21	382×382	40×40	40×40	21×21	401×401	59×59	77×77
20	22×22	422×422	42×42	42×42	22×22	442×442	62×62	81×81

Note that $\mathbf{q}_{(1\times M)}$ is the row vector of initial probabilities associated with the ZS mode so that the initial state on the TPM corresponds to the value of 1. From Equation (13), it follows that the initial state is given by

$$\begin{aligned}
&\text{IRR1: } \mathbf{q}_{(1\times M)} = (1\ 0\ 0\ \dots\ 0) \text{ i.e. the } 1^{\text{st}} \text{ one}\\
&\text{SC1: } \mathbf{q}_{(1\times M)} = (0\ 1\ 0\ \dots\ 0) \text{ i.e. the } 2^{\text{nd}} \text{ one}\\
&\text{IRR2, IRR3, IRR4: } \mathbf{q}_{(1\times M)} = (0\ 0\ \dots\ 1_{\frac{(\tau+1)}{2}}\ \dots 0\ 0) \text{ i.e. the } \left(\tfrac{\tau+1}{2}\right)^{\text{th}} \text{ one}\\
&\text{SC2, SC3, SC4: } \mathbf{q}_{(1\times M)} = (0\ 0\ \dots 0\ 1_{(\tau+1)}\ \dots 0) \text{ i.e. the } (\tau+1)^{\text{th}} \text{ one}
\end{aligned} \tag{14}$$

In SS, the vector $\mathbf{q}$ is replaced by a vector $\mathbf{s}$, i.e. the SS initial probability vector given by

$$\boldsymbol{\xi} = \mathbf{s}_{(1\times M)} = (s_1\ s_2\ \dots\ s_M) \tag{15}$$

where the sum of the elements in Equation (15) sum to unity. Champ[24] showed that when $\mathbf{Q_0}$ is obtained from $\mathbf{Q}(0)$ (i.e. $\delta = 0$) after diving each element by its corresponding row sum, then $\mathbf{s}_{(1\times M)}$ is a vector such that $\mathbf{s} = \mathbf{Q_0}'\mathbf{s}$ subject to $\sum_{i=1}^{M} s_i = 1$.

For illustration purpose, in Table X we give the compound patterns of the eight schemes in Table I when $H \leq 5$ with charting regions in Figure 1.

Table X: Compound patterns[1] of the Markov chain imbedding technique for the *1-of-1* or *2-of-*(*H*+1) IRR and Synthetic-$\bar{X}$ charts when $H \leq 5$

H	IRR1 / SC1	IRR2 / SC2	IRR3 / SC3	IRR4 / SC4
1	E, UU	E, AA, **±A** DD, **±D**	E, AA, **±A** DD, **±D**	E, AA, **±A** DD, **±D**
2	UOU	AOA, ADA, **±OA** DOD, DAD, **±OD**	AOA, **±OA** DOD, **±OD**	ABA, **±BA** DCD, **±CD**
3	UOOU	AOOA, AODA, ADOA, **±OOA** DOOD, DOAD, DAOD, **±OOD**	AOOA, **±OOA** DOOD, **±OOD**	ABBA, **±BBA** DCCD, **±CCD**
4	UOOOU	AOOOA, AOODA, AODOA, ADOOA, **±OOOA** DOOOD, DOOAD, DOAOD, DAOOD, **±OOOD**	AOOOA, **±OOOA** DOOOD, **±OOOD**	ABBBA, **±BBBA** DCCCD, **±CCCD**
5	UOOOOU	AOOOOA, AOOODA, AOODOA, AODOOA, ADOOOA, **±OOOOA** DOOOOD, DOOOAD, DOOAOD, DOAOOD, DAOOOD, **±OOOOD**	AOOOOA, **±OOOOA** DOOOOD, **±OOOOD**	ABBBBA, **±BBBBA** DCCCCD, **±CCCCD**

The breakdown of these compound patterns is done in Table XI by first defining the absorbing states and then obtaining the corresponding non-absorbing states from these. Then Table IX and Equations (10) to (13) are used to construct the TPMs in Table XII for H = 1 and 5. The construction of the TPMs of the other values of H follows in a similar manner.

References

1. Celano G, Costa AFB, Fichera S. Statistical design of variable sample size and sampling interval $\bar{X}$ control charts with run rules. *International Journal of Advanced Manufacturing Technology* 2006; **28**(6-7): 966-977.
2. Reynolds Jr. MR, Arnold JC. EWMA control charts with variable sample sizes and variable sampling intervals. *IIE Transactions* 2001; **33**: 511–530.
3. Daudin JJ. Double sampling $\bar{X}$ charts. *Journal of Quality Technology* 1992; **24**(1): 78-87.
4. Koutras MV, Bersimis S, Maravelakis PE. Statistical process control using Shewhart control charts with supplementary runs rules. *Methodology and Computing in Applied Probability* 2007; **9**(2): 207-224.
5. Scariano SM, Calzada ME. The generalized synthetic chart. *Sequential Analysis* 2009; **28**(1): 54-68.
6. Costa AFB. $\bar{X}$ charts with variable sample size and sampling interval. *Journal of Quality Technology* 1997; **29**(2): 197-204.
7. Wu Z, Spedding TA. A synthetic control chart for detecting small shifts in the process mean. *Journal of Quality Technology* 2000; **32**(1): 32-38.
8. Khoo MBC, Castagliola P, Liew JY, Teoh WL, Maravelakis PE. A study on EWMA charts with runs-rules - the Markov chain approach. *Communication in Statistics – Theory and Methods* 2015; Accepted.

[1] The boldfaced simple patterns with a HS feature (i.e. starting with '±') correspond to Ψ, see Table XI.

9. Abbas N, Riaz M, Does RJMM. (2011). Enhancing the performance of EWMA charts. *Quality and Reliability Engineering International* 2011; **27**(6): 821-833.
10. Abbas N, Riaz M, Does RJMM. Enhancing the performance of exponentially weighted moving average charts: Discussion. *Quality and Reliability Engineering International* 2015, DOI: 10.1002/qre.1615.
11. Haq A, Brown J, Moltchanova E. New synthetic EWMA and synthetic CUSUM control charts for monitoring the process mean. *Quality and Reliability Engineering International* 2015, DOI: 10.1002/qre.1747.
12. Balakrishnan N, Koutras MV. Runs and scans with applications. New York: John Wiley & Sons, Inc., 2002.
13. Klein M. Two alternatives to the Shewhart $\bar{X}$ control chart. *Journal of Quality Technology* 2000; **32**(4): 427-431.
14. Acosta-Mejia CA. Two sets of runs rules for the $\bar{X}$ chart. *Quality Engineering* 2007; **19**: 129-136.
15. Khoo MBC, Ariffin KN. Two improved runs rules for the Shewhart $\bar{X}$ control chart. *Quality Engineering* 2006; **18**(2): 173-178.
16. Bourke PD. Detecting a shift in fraction nonconforming using run-length control charts with 100% inspection. *Journal of Quality Technology* 1991; **23**(3): 225-238.
17. Davis RB, Woodall WH. Evaluating and improving the synthetic control chart. *Journal of Quality Technology* 2002; **34**(2): 200-208.
18. Wu Z, Ou YJ, Castagliola P, Khoo MBC. A combined synthetic & X chart for monitoring the process mean. *International Journal of Production Research* 2010; **48**(24): 7423-7436.
19. Shongwe SC, Graham MA. A modified side-sensitive synthetic chart to monitor the process mean. *Quality Technology and Quantitative Management* Submitted.
20. Derman C, Ross SM. *Statistical Aspects of Quality Control*. Academic Press, San Diego, CA, 1997.
21. Machado MAG, Costa AFB. A side-sensitive synthetic chart combined with an $\bar{X}$ chart. *International Journal of Production Research* 2014; **52**(11): 3404-3416.
22. Antzoulakos DL, Rakitzis AC. The revised *m*-of-*k* runs rule. *Quality Engineering* 2008; **20**(1): 75-81.
23. Riaz M, Abbas N, Does RJMM. Improving the performance of CUSUM charts. *Quality and Reliability Engineering International* 2011; **27**(4): 415-424.
24. Champ CW. Steady-state run length analysis of a Shewhart quality control chart with supplementary runs rules. *Communications in Statistics – Theory and Methods* 1992; **21**(3): 765-777.

25. Zhang S, Wu Z. Designs of control charts with supplementary runs rules. *Computers & Industrial Engineering* 2005; **49**(1): 76-97.
26. Machado MAG, Costa AFB. Some comments regarding the synthetic chart. *Communications in Statistic - Theory and Methods* 2014; **43**(14): 2897-2906.
27. Wu Z, Yang W, Jiang W, Khoo MBC. Optimization designs of the combined Shewhart-CUSUM control charts. *Computational Statistics & Data Analysis* 2008; **53**(2): 496-506.
28. Abujiya MR, Farouk AU, Lee MH, Mohamad I. On the sensitivity of Poisson EWMA control chart. *International Journal of Humanities and Management Sciences* 2013; **1**(1): 18-22.
29. Antzoulakos DL, Rakitzis AC. The modified *r* out of *m* control chart. *Communications in Statistics - Simulation and Computation* 2008; **37**(2): 396-408.
30. Low CK, Khoo MBC, Teoh WL, Wu Z. The revised m-of-k runs-rule based on median run length. *Communications in Statistics - Simulation and Computation* 2012; **41**(8): 1463-1477.
31. Fu JC, Lou WYW. *Distribution Theory of Runs and Patterns and Its Applications: A Finite Markov Chain Imbedding Approach.* Singapore: World Scientific Publishing, 2003.